

Full Length Article

Bilirubin-induced neurotoxic and ototoxic effects in rat cochlear and vestibular organotypic cultures

Haibo Ye^{a,1}, Yazhi Xing^{a,1}, Ling Zhang^a, Jianhui Zhang^b, Haiyan Jiang^c, Dalian Ding^{a,c,*}, Haibo Shi^{a,*}, Shankai Yin^a

^a Department of Otorhinolaryngology, Affiliated Sixth People's Hospital of Shanghai Jiaotong University, 600 Yishan Road, Shanghai 200233, PR China

^b Department of Otolaryngology Head and Neck Surgery, The Third People's Hospital of Chengdu, PR China

^c Center for Hearing and Deafness, Department of Communicative Disorders and Sciences State, University of New York at Buffalo, 137 Cary Hall, 3435 Main Street, Buffalo, NY 14214, USA

ARTICLE INFO

Keywords:

Bilirubin
Inner ear
Ototoxicity
Auditory neuropathy
Apoptosis

ABSTRACT

Exposure to high levels of bilirubin in hyperbilirubinemia patients and animal models can result in sensorineural deafness. However, the mechanisms underlying bilirubin-induced damage to the inner ear, including the cochlear and vestibular organs, remain unknown. The present analyses of cochlear and vestibular organotypic cultures obtained from postnatal day 3 rats exposed to bilirubin at varying concentrations (0, 10, 50, 100, or 250 μM) for 24 h revealed that auditory nerve fibers (ANFs) and vestibular nerve endings were destroyed even at low doses (10 and 50 μM). Additionally, as the bilirubin dose increased, spiral ganglion neurons (SGNs) and vestibular ganglion neurons (VGNs) exhibited gradual shrinkage in conjunction with nuclei condensation or fragmentation in a dose-dependent manner. The loss of cochlear and vestibular hair cells (HCs) was only evident in explants treated with the highest concentration of bilirubin (250 μM), and bilirubin-induced major apoptosis most likely occurred via the extrinsic apoptotic pathway. Thus, the present results indicate that inner ear neurons and fibers were more sensitive to, and exhibited more severe damage following, bilirubin-induced neurotoxicity than sensory HC, which illustrates the underlying causes of auditory neuropathy and vestibulopathy in hyperbilirubinemia patients.

1. Introduction

Neonatal hyperbilirubinemia, otherwise known as jaundice, is universal and affects up to 84% of term and late preterm infants in the first week of life (Bhutani and Wong, 2013; Reichman et al., 2015). This disorder is a very frequent occurrence among neonates due to the delayed induction of the glucuronosylation system after birth. Additionally, concurrent factors such as hemolytic conditions, sepsis, breastfeeding, hypoalbuminemia, and/or dehydration may aggravate jaundice (Dennerly et al., 2001; Maisels and McDonagh, 2008; Watson, 2009). Neonatal jaundice is generally modest, of little clinical significance, and self-resolves within a few days after birth but excessive hyperbilirubinemia can be toxic to the developing nervous system and lead to bilirubin-induced neurological dysfunction and kernicterus, which is a type of brain damage. This damage is most likely to manifest in selective brain areas such as Purkinje cells in the cerebellar cortex

and oculomotor nuclei in the brain stem as well as the subthalamic nucleus, hippocampus, and basal ganglia (Ahdab-Barmada and Moossy, 1984; Shapiro and Nakamura, 2001; Watchko, 2006).

The auditory pathway in the central nervous system (CNS) is also highly vulnerable to bilirubin toxicity (Olds and Oghalai, 2015). For example, damage may occur in selective retrocochlear structures within the auditory system, including cranial nerve VIII, brainstem auditory nuclei, and inferior colliculi (Olds and Oghalai, 2015; Watchko, 2016), and specific functional and anatomical deficits have been identified in animal models (Li et al., 2011a, b; Rice and Shapiro, 2006; Shapiro, 1994). Additionally, several *in vivo* studies have reported toxicity in the central auditory system of human subjects with hyperbilirubinemia (Jiang et al., 2007; Oysu et al., 2002; Perlman et al., 1983; Rhee et al., 1999; Sano et al., 2005; Sharma et al., 2006) and it has been confirmed that bilirubin-induced damage in this system may be due to excitotoxicity in neurons (Li et al., 2011a, b; Li et al., 2012; Shi et al.,

* Corresponding authors at: Department of Otorhinolaryngology, Affiliated Sixth People's Hospital of Shanghai Jiaotong University, 600 Yishan Road, Shanghai 200233, PR China.

E-mail addresses: dding@buffalo.edu (D. Ding), haibo99@hotmail.com (H. Shi).

¹ These authors have contributed equally to this work.

2006). Previous findings from our research group indicate that bilirubin can induce neuronal hyperexcitability in the ventral cochlear nucleus and lateral superior olive nucleus by increasing excitatory presynaptic neurotransmitter release (Li et al., 2011a, b; Li et al., 2012; Liang et al., 2017b; Shi et al., 2006). Our group also reported that P/Q-subtype calcium channels are likely to contribute to an early neuronal vulnerability to hyperbilirubinemia in auditory brain regions (Liang et al., 2017a).

Although abnormal otoacoustic emissions (OAEs) have been reported in clinical cases of neonates with hyperbilirubinemia, it remains uncertain whether bilirubin directly damages peripheral auditory organs (Oysu et al., 2002; Sheykholeslami and Kaga, 2000). OAE abnormalities are considered to be evidence of damage to outer hair cells (OHCs) and this procedure is often performed during newborn hearing screenings (Hrncic, 2018). However, morphological evidence from OHC lesions in patients with hyperbilirubinemia are not yet available, even in cases with a severely abnormal or absent auditory brainstem response (ABR) (Rhee et al., 1999; Ye et al., 2012). In sulfa-injected Gunn rats, the administration of bilirubin results in smaller spiral ganglion neuron (SGN) bodies with decreased cellular density and can cause the selective loss of large diameter axons (Belal, 1975; Shaia et al., 2005). Previous studies from our research group observed demyelinating lesions of auditory nerve fibers (ANFs) in the cochlea in conjunction with damage to type I afferent terminals beneath inner hair cells (IHCs) (Ye et al., 2012, 2013). However, all cochlear HCs remained intact in these studies. Taken together, these findings suggest that hyperbilirubinemia may be linked to auditory neuropathy spectrum disorder (ANSO). Interestingly, it has been shown that vestibulopathy is also relatively prevalent in pediatric ANSD as it was reported in 43% of children in a study series and was associated with significant comorbidities, such as neonatal jaundice (Nash et al., 2014).

Cochlear sensory HCs in the organ of Corti, vestibular sensory HCs in the otolith organs and crista of ampullae, and their respective nerve fibers and primary neurons are very similar in terms of anatomy and development (Jeffery and Spoor, 2004). In a variety of different experimental models, both cochlear and vestibular sensory HCs exhibit similar damage following exposure to ototoxic drugs (Dalian et al., 2013; Ding et al., 2011a, b; Ding et al., 2002; Yu et al., 2011, 2015). Moreover, Ozkiraz (Ozkiraz et al., 2012) determined that severe hyperbilirubinemia causes delayed latencies in vestibular-evoked myogenic potential in term newborns. Although these authors proposed that severe hyperbilirubinemia can affect vestibular nuclei and/or the integrity of the inferior vestibular nerve and vestibulospinal tract, they did not investigate whether peripheral vestibular receptors could be also damaged by bilirubin. Thus, to gain novel insights regarding the in vitro neurotoxic and ototoxic effects and mechanisms of bilirubin, cochlear and vestibular explants were treated with various doses of bilirubin in the present study. The explants were examined to determine the bilirubin dose-response curve, assess pathological changes, and identify changes in the expressions of free radicals and cellular apoptotic signals to clarify further the effects of hyperbilirubinemia in the inner ear.

2. Materials and methods

2.1. Animal procedures

All experimental procedures regarding the care and use of rat pups were reviewed and approved by the Animal Ethics Committee of Shanghai Sixth People's Hospital. All efforts were made to minimize possible pain and discomfort of the animals during the experimental procedures.

2.2. Collagen gel and culture medium preparations

Collagen gel was prepared to provide an appropriate environment

for the explants to grow. The preparations of collagen gel and serum-free medium have been described in detail in previous publications from our research group (Dalian et al., 2013; Ding et al., 2011a, 2002; Fu et al., 2013; Gao et al., 2017; Yu et al., 2011). Briefly, rat tail collagen (Type 1, BD Biosciences; Bedford, MA) was gently mixed with 10 × Eagle's Basal Medium (BME; B9638, Sigma; St. Louis, MO) and 2% sodium carbonate at a ratio of 9:1:1 prior to use. Next, 10 µl of collagen gel was placed in the center of a 35 mm culture dish (Falcon 353001, Northbrook, IL) for 30 min to let the collagen solidify and then 1.3 ml of serum-free medium was applied to cover the collagen. The serum-free medium used in the present study contained 2 g of bovine serum albumin (BSA; A-4919, Sigma; St. Louis, MO), 2 ml of Serum-Free Supplement (I-1884, Sigma; St. Louis, MO), 4.8 ml of 20% glucose (G-2020, Sigma; St. Louis, MO), 0.4 ml of penicillin G (P-3414, Sigma; St. Louis, MO), 2 ml of 200 mM glutamine (G-6392, Sigma; St. Louis, MO), and 190.8 ml of 1 × BME (B-1522, Sigma; St. Louis, MO).

2.3. Cochlear and vestibular explant preparations

Rat pups (postnatal day 3) were used to obtain explant cultures. After quickly removing the temporal bone, cochlear and vestibular explants were dissected out and placed in ice-cold Hank's Balanced Salt Solution (HBSS); the micro-dissection techniques are described in previous publications from our research group (Dalian et al., 2013; Ding et al., 2012b; Gao et al., 2017; Yu et al., 2015). Briefly, the membranous labyrinth was exposed by removing the bony shell of the inner ear. After separately dissecting out the cochlear basilar membrane that connects the SGNs and the macula of the utricle that connects the superior vestibular ganglion neurons (VGNs), the tectorial membrane and otolithic membrane were gently pulled out and the explants were placed on the collagen gel covered by serum-free medium. The cochlear and vestibular explants were incubated at 37 °C in 5% CO₂ (#3029, Forma Scientific; Marietta, OH) for 1 h to allow the explants to grow on the surface of collagen gel. Then an additional 0.7 ml of medium was added to the culture dish to allow the explants to grow overnight in the same incubator.

2.4. Bilirubin treatment

To determine the dose-response curve for the effects of bilirubin on HCs and GNs in the cochlear and vestibular organs, the culture medium was replaced with freshly prepared serum-free medium containing bilirubin at varying concentrations (0, 10, 50, 100, or 250 µM; n = 6 per concentration) for 24 h on the second day. Specimens treated with either a 0 or 250 µM dose of bilirubin for 12 or 24 h were used to analyze apoptotic activity; six samples were obtained from each experimental group.

2.5. Histology

For histological analysis, the cochlear and vestibular explants were fixed with 10% formalin for 3 h at the end of the treatment. Anti-β-tubulin III antibody, phalloidin, and ToPro-3 were applied to the fixed tissues to label nerve fibers and GNs, the stereocilia and the cuticular plate of the HC, and the nuclei, respectively; the steps for this triple-labeling procedure have been described in detail in previous publications from our research group (Dalian et al., 2013; Ding et al., 2011a; Li et al., 2015). Briefly, the specimens were incubated with mouse anti-β-tubulin III antibody (1:100; TUJ1, MMS-435 P, BioLegend; San Diego, CA) that was diluted in blocking solution containing 1% Triton X-100 and 5% goat serum in 0.1 M phosphate-buffered saline (PBS) for 24 h at 4 °C. After rinsing the specimens with 0.1 M PBS, they were incubated in either a goat anti-mouse secondary antibody conjugated with TRITC (1:200; T5393, Sigma) or a goat anti-mouse secondary antibody conjugated with Alexa Fluor 488 (1:200; ab150113; San Francisco, CA) in a blocking solution for 2 h at room temperature. Next, the specimens

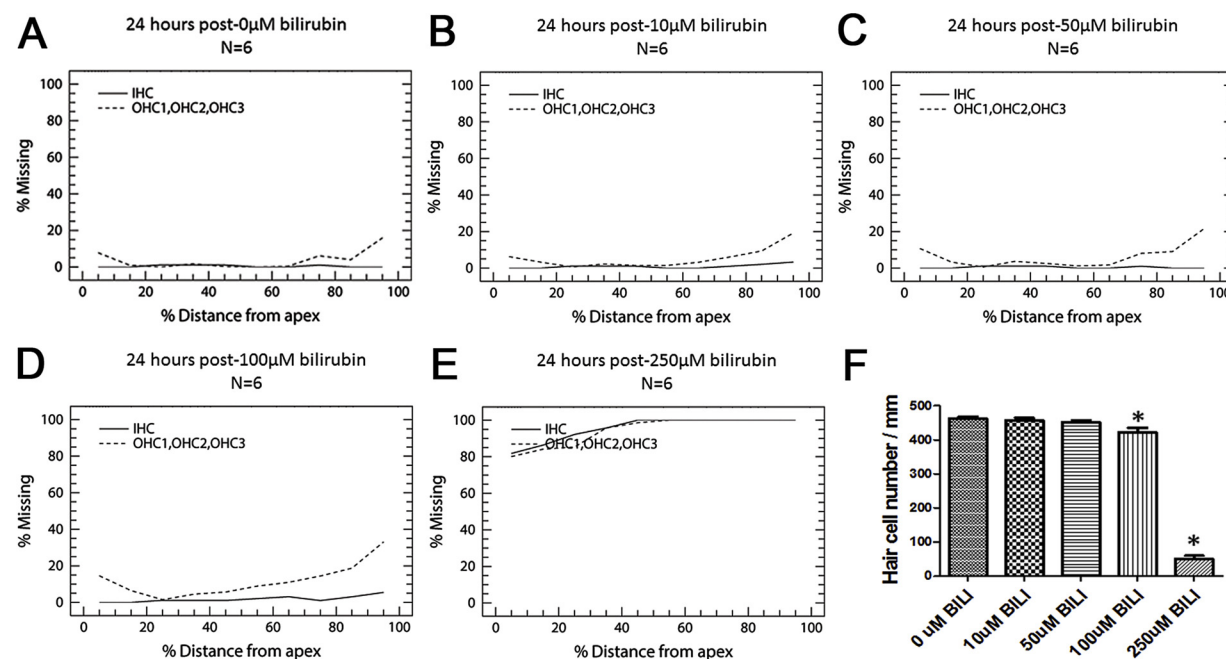


Fig. 1. Grouped cochleograms showing the percentage loss of IHCs (solid line) and OHCs (dashed line) induced by bilirubin treatment for 24 h at various doses (0, 10, 50, 100, and 250 μ M; A–F). In the control, 10 μ M, and 50 μ M bilirubin treatment groups, most OHCs and IHCs maintained normal morphological structure with no obvious loss of HCs, except for in the hook region (A–C). In the 100 μ M group, there was a small increase in the loss of OHCs in the hook region but most HCs remained intact (D). Increasing the bilirubin dose to 250 μ M destroyed 100% of OHCs and IHCs in the basal turn and more than 80% of HCs in the apical turn (E). Compared to the normal control group, there were significant differences in HC density when the bilirubin dose exceeded 100 μ M (F; $p < 0.05$).

were again rinsed with 0.1 M PBS and stained with either Alexa Fluor 488- or Alexa Fluor 555-conjugated phalloidin (1:100, Cytoskeleton PHDG1-A or Cytoskeleton PHDH1-A, Denver, CO) while the nuclei were counterstained with 1 μ M of ToPro-3 (T3605, ThermoFisher; Waltham, MA) for 60 min.

After being mounted in glycerin and coverslipped, the specimens were evaluated with a fluorescent microscope ($400\times$, Zeiss Axioskop; Dublin, CA) to quantify the HCs and a confocal microscope (Zeiss LSM-510) to further evaluate the HCs. Neuronal assessments were conducted using appropriate filters for TRITC (absorption: 544 nm, emission: 572 nm), Alexa Fluor 488 (absorption: 495 nm, emission: 519 nm), Alexa Fluor 555 (absorption: 555 nm, emission: 565 nm), and To-Pro-3 (absorption: 642 nm, emission: 661 nm). All images were evaluated with the Zeiss LSM Image Examiner and post-processed with Adobe Photoshop software. The triple-stained specimens were assessed to image and quantify cochlear and vestibular HCs, cochlear and vestibular GNs, and their nerve fibers.

2.6. Quantification of cochlear HCs

Cochlear explants were stained with Alexa Fluor 488-conjugated phalloidin and then examined using a microscope at $400\times$ magnification (Zeiss LSM-510) for the quantification of HCs. IHCs and OHCs were counted over 0.24 mm intervals along the entire cochlea from the apical turn to the basal turn; all data are presented as the percent distance from the apex to the base. HCs were considered to be missing or lost if the stereocilia and cuticular plate were absent. All data were analyzed in a custom computer program designed to generate a cochleogram that could be compared to those generated from normal SASCO Sprague-Dawley rats. Each dataset was averaged from n samples from each experimental group (Ding et al., 2011a; Li et al., 2015; Wang et al., 2014; Yu et al., 2015).

2.7. Quantification of HC density in vestibular end-organs

To evaluate bilirubin toxicity in terms of the loss of vestibular HCs,

the HCs were counted in multiple regions ($141 \mu\text{m}^2$) under a microscope; HC density values are shown as the number of HCs per 0.02 mm^2 . Three to five locations from each specimen were measured and the average value of these locations was the HC density included in the analyses. All analyses were conducted using GraphPad Prism 5 (Graphpad Software; San Diego, CA, USA), as previously described (Dong et al., 2014; Zhou et al., 2009), and all data were statistically analyzed using one-way analysis of variance (ANOVA) tests followed by Newman-Keuls post hoc analyses. All tests were two-sided and p values < 0.05 were considered to indicate statistical significance.

2.8. Measurements of cell size in SGNs and VGNs

Following bilirubin treatment, SGNs and VGNs were stained with the anti- β -tubulin III antibody for neuronal evaluations with a confocal Zeiss LSM Image Examiner, as previously described (Fu et al., 2013; Wei et al., 2010; Yu et al., 2015). Briefly, a z-stack of confocal images at $630\times$ magnification was collected and merged. To avoid subjective biases, the number of layers was maximized to obtain the largest gross sectional area of each GN and the overlap among the different GNs was minimized. A polygon was drawn around the perimeter of all distinguishable GNs and the area was automatically calculated using the Zeiss LSM Image Examiner (version: 4.0.0.91). All data were evaluated for statistical significance with SigmaStat (version: 3.5.0.54).

2.9. Caspase labeling

To analyze the effects of the activations of different caspases on bilirubin-induced activity, CaspGLOW Red Active caspase-8, caspase-9, and caspase-3 Staining Kits (K188, K118, K183, BioVision; Milpitas, CA) were used to test two initiators (caspase-8 and caspase-9) and one executioner (caspase-3) in cochlear and vestibular explants treated with 250 μ M bilirubin for 12 and 24 h; samples that were not treated with bilirubin were used as a control (Ding et al., 2007; Dong et al., 2014; Li et al., 2015; Yu et al., 2011). Briefly, the three abovementioned caspase detection kits were applied to the explant culture medium at a dilution

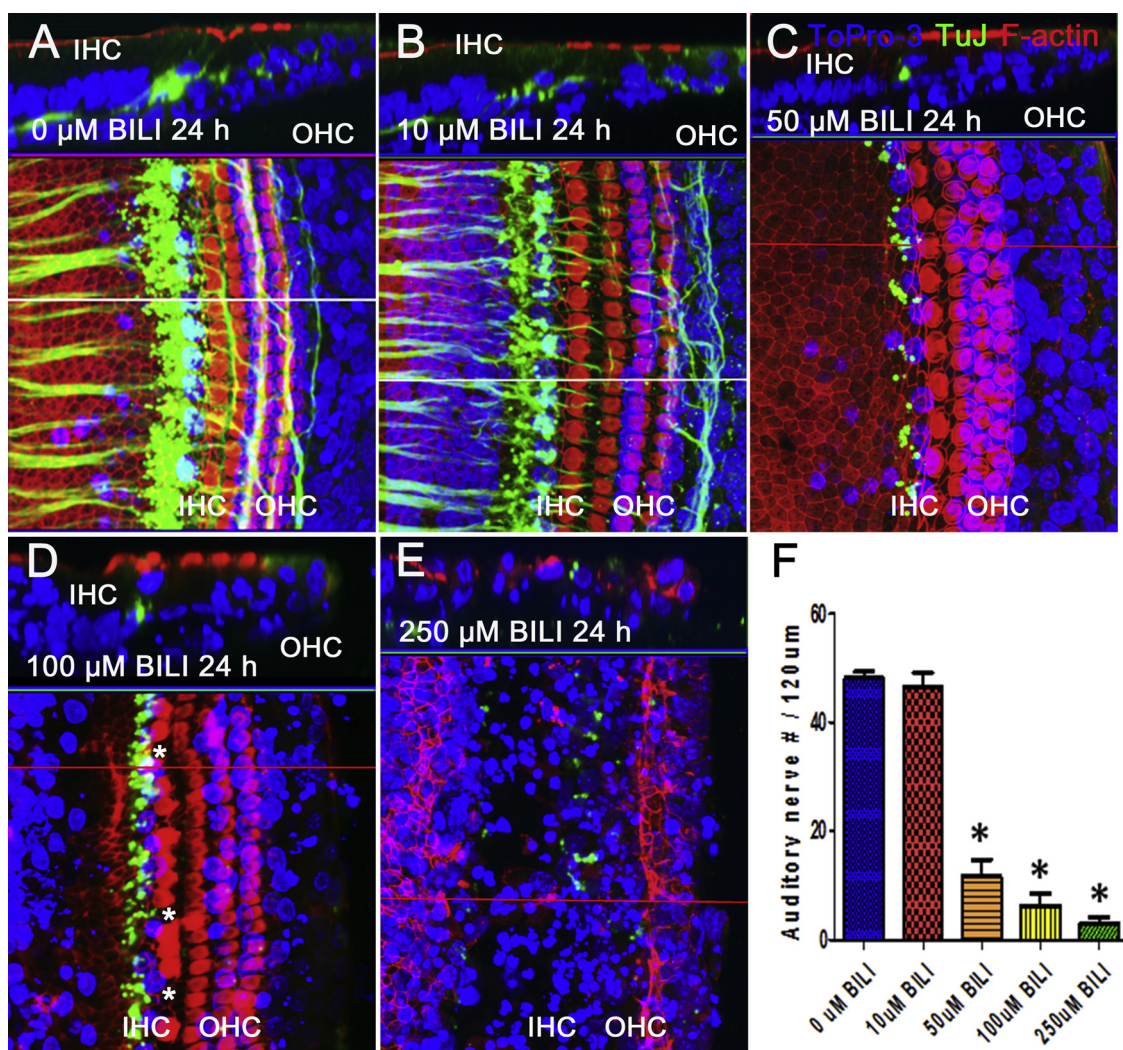


Fig. 2. Early bilirubin-induced damage to ANFs and their synapses. Alexa Fluor 488-labeled β -tubulin protein (TuJ) expression was intense in the ANFs and their terminals in the normal control and 10 μ M bilirubin-cultured cochlear explants (A–B). ANFs and their synapses were completely destroyed when the dose of bilirubin exceeded 50 μ M (C–E). There was a significant reduction in auditory nerve density when the dose of bilirubin exceeded 50 μ M (F). Cochlear HCs exhibited a normal appearance until the dose of bilirubin reached 100 μ M (A–D). The highest dose of bilirubin (250 μ M) destroyed most cochlear HCs (E; $p < 0.05$). F-actin on stereocilia and cuticular plate of HCs were stained with Fluor 555-conjugated phalloidin (shown in red). Auditory nerve fibers were labeled with β -tubulin (shown in green). Nuclei were stained with ToPro-3 (shown in blue). Arrowhead indicates the location of the IHCs, arrow indicates the location of the OHCs, and the asterisk indicates the lost IHCs.

of 1:100 for 1 h prior to the end of the experiments. All specimens were fixed in 10% formalin in PBS for 3 h after being rinsed with PBS, and Alexa Fluor 488-conjugated phalloidin and To-Pro-3 were used to label the HCs and the nuclei, respectively. Finally, the samples were mounted in glycerin and examined using a confocal microscope with the appropriate filters.

3. Results

3.1. Bilirubin-induced cochlear HC degeneration

Grouped cochleograms for each experimental condition revealed that the pattern and extent of lost HCs due to bilirubin treatment for 24 h were dose-dependent (0, 10, 50, 100, and 250 μ M; Figs. 1A–F). The normal control group was cultured with standard serum-free medium in the absence of bilirubin and most OHCs and IHCs were intact, except for in the hook region that was mechanically damaged by cochlear dissections or sample preparations (Fig. 1A). In the 10 and 50 μ M bilirubin groups, most OHCs and IHCs maintained their normal morphological structure without any missing HCs, except for the hook region

(Fig. 1B–C). At a bilirubin dose of 100 μ M, very few missing OHCs were detected in the hook region and most HCs remained intact (Fig. 1D). At a bilirubin dose of 250 μ M, 100% of OHCs and IHCs in the basal turn were destroyed and more than 80% of HCs were missing in the apical turn (Fig. 1E). For quantitative analyses of the HC count data, the cochleogram program was used to compute the number of lost HCs in 10% intervals along the entire length of the cochlea. The mean density values of OHCs and IHCs in the region from 10 to 90% were also determined. The HC density in groups that received a bilirubin dose exceeding 100 μ M significantly differed from the HC density in the normal control group ($p < 0.05$; Fig. 1F). Taken together, these results indicate that the bilirubin-induced destruction of cochlear HCs occurred only at the highest dose (250 μ M) and that OHC damage may manifest slightly earlier than IHC damage.

3.2. Early bilirubin-induced damage to the ANFs and their synapses

To determine the earliest bilirubin-induced damage in the organ of Corti, the cochlear HCs, ANFs, and their synapses were evaluated (Fig. 2). Fig. 2A–E depict a series of representative photomicrographs

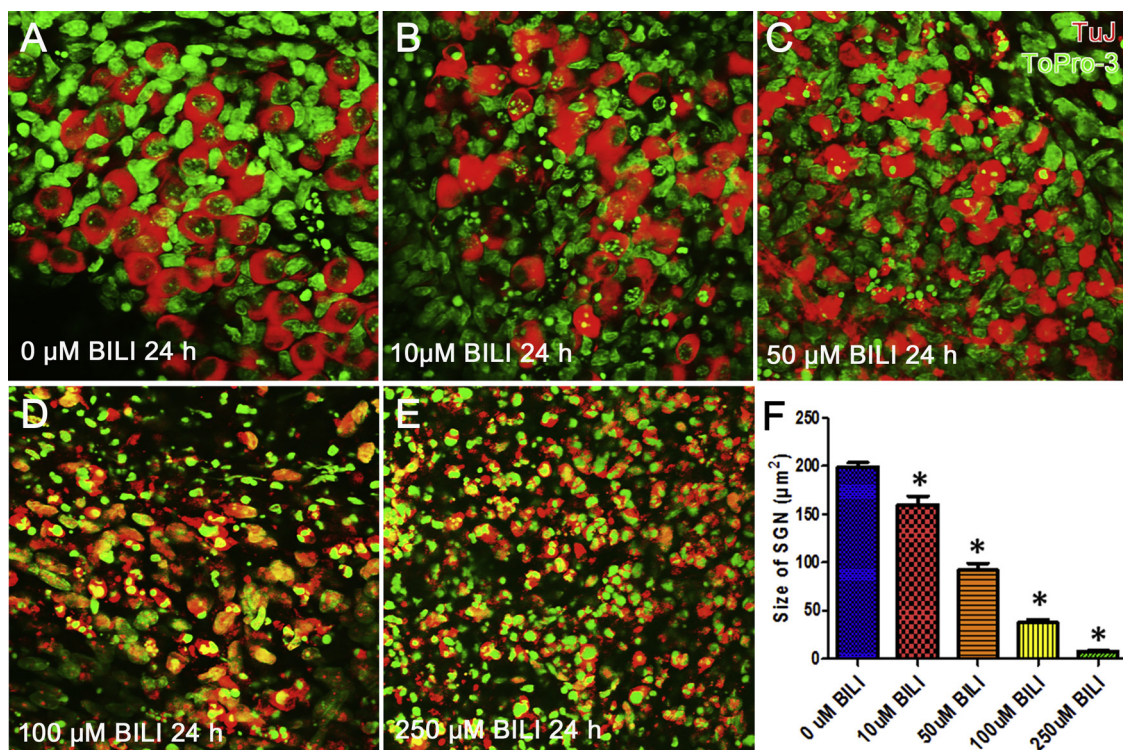


Fig. 3. Bilirubin-induced shrinkage and condensation of nuclear and supporting cells in SGNs. The SGNs in the normal control cochleae at 24 h after culture exhibited large oval-shaped somas with large, round, and homogeneously-labeled nuclei (A). The average size of the normal SGNs in the control group was $199 \mu\text{m}^2$ at 24 h after culturing with standard serum-free medium without bilirubin (F). As the bilirubin dose increased, the SGNs exhibited marked shrinkage in conjunction with nuclei condensation or fragmentation in a dose-dependent manner (B–E). Statistical analyses revealed significant differences in SGN size among the experimental conditions (F; $p < 0.0001$). Spiral ganglion neurons were shown in red by β -tubulin (TuJ) immunostaining. Nuclei were shown in green by ToPro-3 staining.

that illustrate the conditions of bilirubin-treated cochlear explants at different doses (0, 10, 50, 100, and 250 μM). Alexa Fluor 488-labeled β -tubulin proteins were intensely expressed in the ANFs and their terminals in the normal control and 10 μM bilirubin-cultured cochlear explants (Fig. 2A–B). However, ANFs and their synapses were completely destroyed when the dose of bilirubin exceeded 50 μM (Fig. 2C–E). Compared to the ANF density in the control group, there was a significant reduction in ANF density when the bilirubin dose exceeded 50 μM ($p < 0.0001$; Fig. 2F). Alexa Fluor 555-conjugated phalloidin labels F-actin, which was heavily expressed in the stereocilia bundles and the circumferential ring surrounding the cuticular plate of the HCs. The cochlear HCs maintained a normal density until the dose of bilirubin reached 100 μM (Fig. 2A–D) whereas the highest dose of bilirubin (250 μM) destroyed most cochlear HCs (Fig. 2E). The above results indicate that bilirubin-induced ANF damage appeared earlier and was more severe than that observed in cochlear sensory HCs.

3.3. Early bilirubin-induced damage in SGNs

To determine the degree of bilirubin-induced shrinkage in cochlear SGNs, which is a typical characteristic of apoptosis, neurons were immunostained with Alexa Fluor 555-labeled β -tubulin; the sizes of the SGNs are shown in Fig. 3. The SGNs in the normal control cochleae at 24 h after culture exhibited large oval-shaped somas with large, round, and homogeneously-labeled nuclei (Fig. 3A). The average size of the normal SGNs was $199 \mu\text{m}^2$ at 24 h after culturing in standard serum-free medium in the absence of bilirubin (Fig. 3F). As the bilirubin dose increased, the SGNs exhibited marked shrinkage in conjunction with nuclei condensation or fragmentation in a dose-dependent manner (Figs. 3B–E). At 24 h after treatment with 10, 50, 100, or 250 μM bilirubin, the average sizes of the SGNs gradually decreased to 159.65, 91.94, 37.24, and $7.47 \mu\text{m}^2$, respectively (Fig. 3F). Statistical analyses

revealed significant differences among the sizes of the SGNs in the above experimental conditions ($p < 0.0001$). When these data were compared to the dose-response relationship of damage in the cochlear HCs (Figs. 1–2), it was obvious that the bilirubin-induced neurotoxicity was more severe in cochlear SGNs than in cochlear HCs.

3.4. Bilirubin-induced damage in vestibular end-organs

Fig. 4 shows a series of representative confocal photomicrographs that illustrate the conditions of vestibular sensory HCs and vestibular type I synapses in the macula of the utricle in the control group (0 μM) and bilirubin-treated groups (10, 50, 100, and 250 μM). Fig. 4A–E show the flat and Z-plane sectioning images from the horizontal surface preparations of the macula of the utricle. The stereocilia bundles and cuticular plate of the vestibular HCs were stained with Alexa Fluor 555-conjugated phalloidin while the vestibular nerve endings were immunolabeled with Alexa Fluor 488-labeled β -tubulin (Fig. 4A–E). The phalloidin-positive stereocilia on the vestibular HCs were normal in the control and 10–100 μM bilirubin groups (Fig. 4A–D) and only vestibular HCs in the 250 μM bilirubin group exhibited damage after 24 h of treatment (Fig. 4E). In contrast, the destruction of vestibular type I nerve endings began at 24 h after treatment with 10 μM bilirubin (Fig. 4B). When the dose of bilirubin was 50 μM and higher, all vestibular type I nervous synapse terminals were completely destroyed (Fig. 4C–E).

Statistical analyses of vestibular HC density revealed that vestibular HCs were missing only after the highest dose (250 μM) in bilirubin-treated vestibular explants. In contrast, the destruction of vestibular type I synapses occurred at the lowest bilirubin dose (10 μM). Additionally, the density of chalice-shaped type I afferent terminals significantly differed among the experimental groups ($p < 0.0001$; Fig. 4F). The cilia and nuclei of the vestibular HCs were destroyed

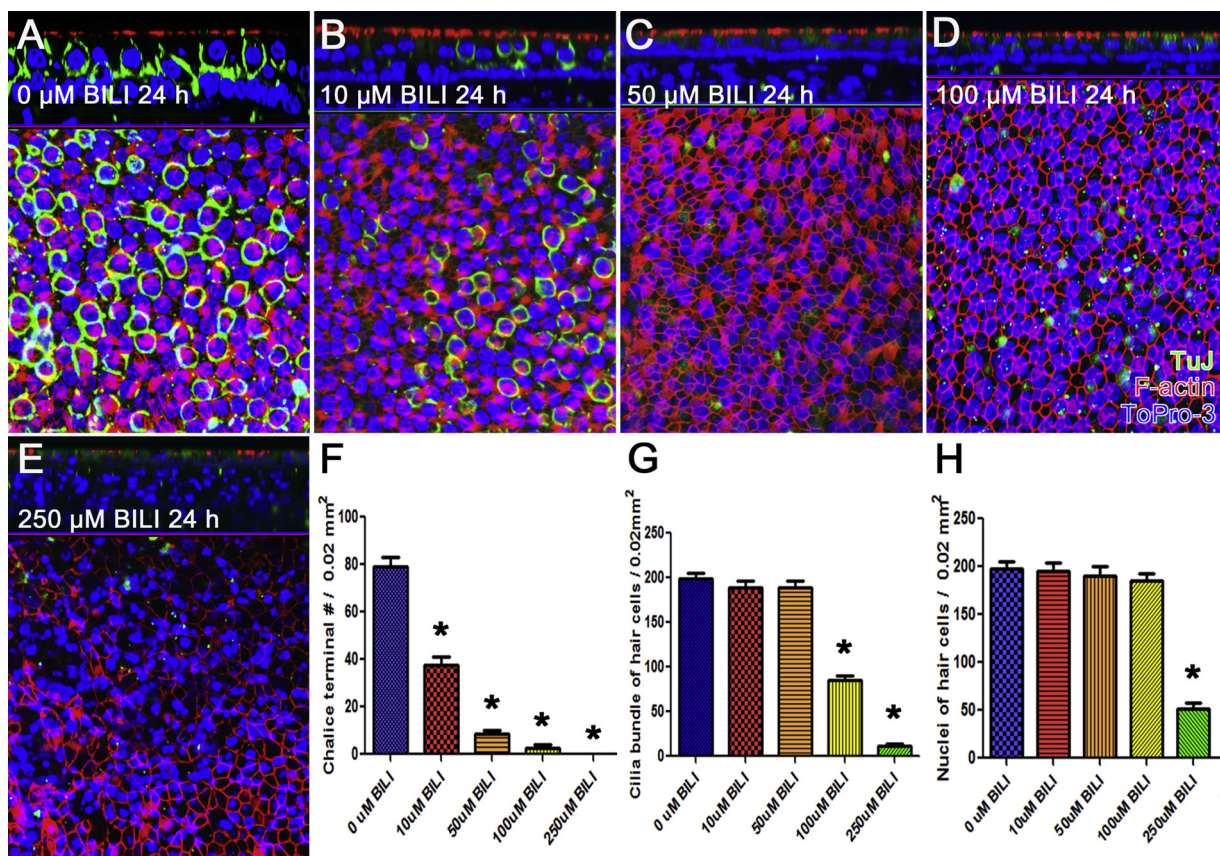


Fig. 4. Bilirubin-induced degeneration in vestibular nerve fibers and HCs in the macula of the utricle. Phalloidin-positive cilia bundles were present in vestibular HCs in the normal control and 10–100 μM bilirubin groups (A–D) but the vestibular HCs were damaged by treatment with 250 μM bilirubin for 24 h (E). All terminals in vestibular type I synapses were completely destroyed when the dose of bilirubin was 50 μM and higher (4C–E). Statistical analyses of vestibular HC density revealed that the loss of vestibular HCs only occurred following treatment with 250 μM bilirubin and that the destruction of vestibular type I synapses occurred following treatment with 10 μM bilirubin. The density of chalice-shaped type I afferent terminals significantly differed among the experimental conditions (F; $p < 0.0001$). The cilia of vestibular HCs exhibited a greater degree of earlier destruction than nuclei in the vestibular HCs (G–H; $p < 0.0001$). F-actin on stereocilia was stained with Fluor 555-conjugated phalloidin (red). Terminals of vestibular nerve fibers were labeled with β -tubulin (green). Nuclei were stained with ToPro-3 (blue). Arrows indicate the chalice-shaped afferent terminals surrounding the macula type I HCs.

following treatment with 100 and 250 μM bilirubin, respectively, which suggests that the cilia were more sensitive to bilirubin-induced toxicity than the nuclei of vestibular HCs ($p < 0.0001$; Fig. 4G–H).

3.5. Early bilirubin-induced damage in VGNs

Fig. 5 illustrates the typical status of VGNs in the control vestibular explants (0 μM; Fig. 5A) and in cultures treated with 10, 50, 100, or 250 μM bilirubin for 24 h. After the VGNs were stained with Alexa Fluor 555-labeled β -tubulin and the nuclei were stained with To-Pro-3, the sizes of the VGNs were measured. At 24 h after culturing, the VGNs that were not treated with bilirubin appeared normal (Fig. 5A) and their average size was $314.22 \mu\text{m}^2$ (Fig. 5F). After treatment with 10 μM bilirubin, the VGNs exhibited significant shrinkage and their average size decreased to $195.89 \mu\text{m}^2$ (Fig. 5B and F). When the doses of bilirubin increased to 50 and 100 μM, the shrinkage of the vestibular neurons became more pronounced and their average sizes decreased to $70.33 \mu\text{m}^2$ and $51 \mu\text{m}^2$, respectively (Fig. 5C, D, and F). The highest dose of bilirubin (250 μM) significantly shrunk the VGNs and surrounding supporting cells such that the average size of the VGNs decreased to $12.83 \mu\text{m}^2$ (Fig. 5F). Statistical analyses revealed significant differences in VGN sizes among the experimental groups ($p < 0.0001$) and, similar to the early bilirubin-induced damage in cochlear SGNs, the VGNs were also more sensitive to bilirubin than the vestibular sensory HCs.

3.6. Bilirubin-induced caspase activations

Because the bilirubin-induced morphological features of apoptosis (i.e., soma shrinkage, nuclear condensation, and fragmentation) precede cell destruction, it is possible that programmed cell death is initiated by either extrinsic or intrinsic apoptotic pathways. To gain insight into the precise mechanisms that trigger cell apoptosis, the time courses of the expressions of caspase-8, caspase-9, and caspase-3 at 12 or 24 h after treatment with either 0 or 250 μM bilirubin were examined. The photomicrographs in Figs. 6, 7 and 8 show a series of activations for an extrinsic apoptotic marker (initiator caspase-8), an intrinsic apoptotic marker (initiator caspase-9), and a downstream executioner (caspase-3), respectively, in control cultures and cultures treated with 250 μM bilirubin for 12 or 24 h.

Caspase-8, -9, and -3 were all absent in the normal control cochlear and vestibular sensory epithelium and peripheral GNs (Figs. 6A–D, 7 A–D, and 8 A–D, respectively). However, at 12 h after treatment with 250 μM bilirubin, caspase-8 was intensely expressed in the cochlear and vestibular GNs but did not show activation in the cochlear and vestibular sensory HCs (Fig. 6F and H). At 24 h after treatment with 250 μM bilirubin, caspase-8 activation was detected in all cochlear and vestibular sensory HCs and their peripheral GNs (Fig. 6I–L). Caspase-9 activation was not observed in either the cochlear or vestibular cells in the normal control cultures or at 12 h after treatment with 250 μM bilirubin (Fig. 7A–H) whereas this protein was expressed in all cochlear and vestibular sensory HCs and their GNs at 24 h after treatment with

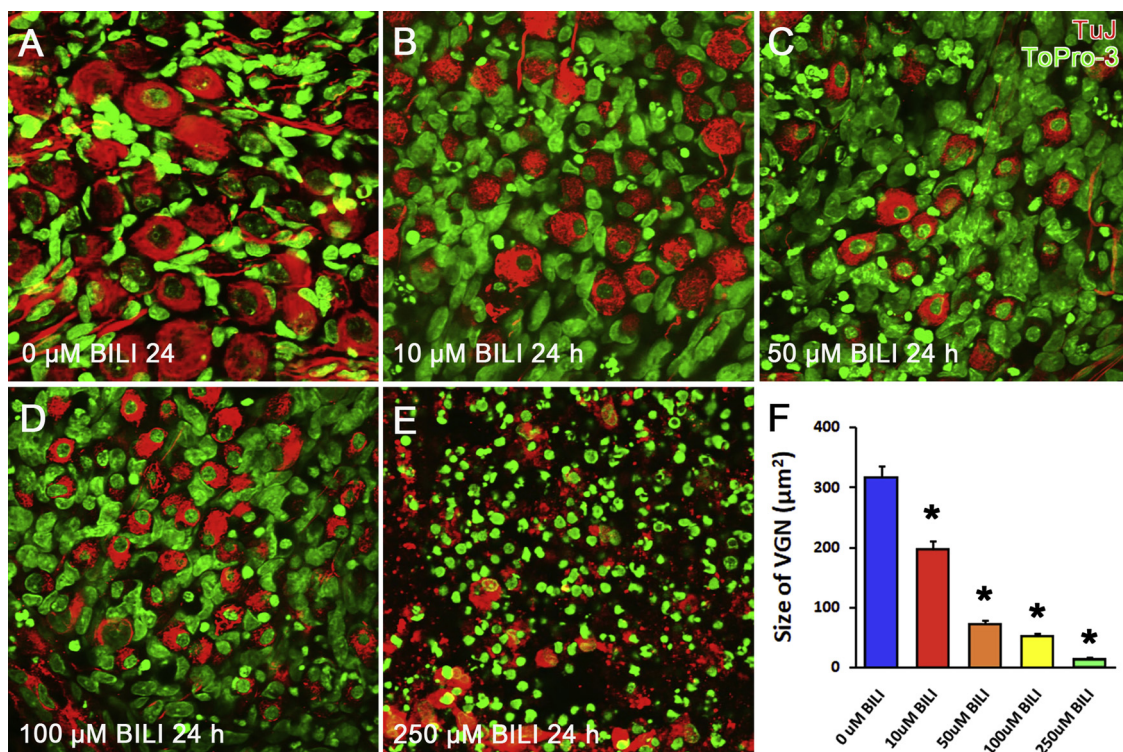


Fig. 5. Bilirubin-induced nuclear shrinkage and condensation in VGNs. In the control group, the VGNs were normal and the average size of the normal VGNs was $314.22 \mu\text{m}^2$ (A–F). When the doses of bilirubin increased to 10, 50, 100, and 250 μM , the shrinkage of the vestibular neurons became more pronounced and the average sizes of the VGNs were reduced to 195.89, 70.33, 51, and $12.83 \mu\text{m}^2$, respectively (B–F). Statistical analyses revealed significant differences in the average size of the VGNs among the experimental conditions (F; $p < 0.0001$). Vestibular neuron and nerve fibers were labeled with β -tubulin (red). Nuclei were stained with ToPro-3 (green).

250 μM bilirubin (Fig. 7I–L). Similar to the activation of the initiator caspase-8, the executioner caspase-3 was detected but only appeared in SGNs and VGNs and not cochlear and vestibular sensory HCs at 12 h after treatment with 250 μM bilirubin (Fig. 8F–H). At 24 h after treatment with 250 μM bilirubin, caspase-3 activation was detected in all cochlear and vestibular sensory HCs and their peripheral GNs (Fig. 8I–L).

4. Discussion

The present study was the first to investigate the potential neurotoxic effects of bilirubin in cochlear and vestibular organotypic culture systems. The data presented here clearly demonstrate that cochlear and vestibular SGNs and ANFs were more sensitive to bilirubin-induced neurotoxicity and experienced more severe effects than bilirubin-induced ototoxicity in the cochlear and vestibular sensory HCs. In addition to kernicterus caused by hyperbilirubinemia, the most toxic effects of bilirubin are associated with neurotoxicity. Over the past century, bilirubin-induced toxicity has been extensively studied in the CNS and many studies have shown that specific neurons in selective brain regions, particularly auditory neurons in the brainstem and inferior colliculus, are the primary targets of bilirubin neurotoxicity (Ahlfors and Shapiro, 2001; Shapiro and Popelka, 2011; Watchko, 2006). Because bilirubin-induced hearing impairments are so common and are relatively severe compared to those observed in other systems, it has been suggested that the ABR be used as an objective test for judging bilirubin neurotoxicity (Gupta and Mann, 1998; Shapiro and Popelka, 2011). Bilirubin administration can quickly cause significant changes in the ABR but usually does not interfere with OAEs or cochlear microphonics (CM) and, thus, several previous studies have suggested that the effects of bilirubin on the auditory system initially occur in the brainstem (Ye et al., 2012, 2013). Subsequently, this damage is thought to progress to

cranial nerve VII as well as higher nerve centers (Rance and Starr, 2015). However, simultaneous observations of cochlear bioelectricities and the ABR have revealed that threshold elevation is detected in both the cochlear compound action potential (CAP) and ABR as early as 1 h after bilirubin treatment. The functional changes in CAP are consistent with damage to the auditory synapses beneath the IHCs as well as the demyelination of SGNs and their ANFs in the cochlea (Ye et al., 2012). Therefore, the toxic effects of bilirubin in the auditory system not only cause damage to auditory neurons in the brainstem but also destroy peripheral SGNs and nerve endings in the cochlea.

The injury patterns and pathological mechanisms underlying hyperbilirubinemia have yet to be determined but this disorder is highly linked to ANSD, which is characterized by an absent ABR, normal OAEs and/or CM, elevated auditory sensitivity, and word discrimination disproportional to the pure tone audiogram (Rance and Starr, 2015; Starr et al., 1996). It is estimated that approximately one-third to one-half of ANSD cases have a history of severe hyperbilirubinemia and/or anoxia during the neonatal period (Madden et al., 2002; Rance, 2005; Rance et al., 1999; Saluja et al., 2010). Starr has addressed the clinical and pathophysiological features of auditory neuropathy that distinguish site(s) of dysfunction and described the diagnostic criteria for the following: (i) presynaptic disorders affecting IHCs and ribbon synapses; (ii) postsynaptic disorders affecting unmyelinated auditory nerve dendrites; (iii) postsynaptic disorders affecting auditory ganglion cells and their myelinated axons and dendrites; and (iv) central neural pathway disorders affecting the auditory brainstem (Moser and Starr, 2016; Rance and Starr, 2015). In the present in vitro study, relatively low doses of bilirubin (10 and 50 μM) had a greater destructive effect on SGNs, ANFs, and loss of Type I afferent endings beneath IHCs while sparing cochlear sensory HCs. This phenomenon is consistent with previous in vivo findings from our research group showing that systemic bilirubin treatment does not alter distortion product OAEs

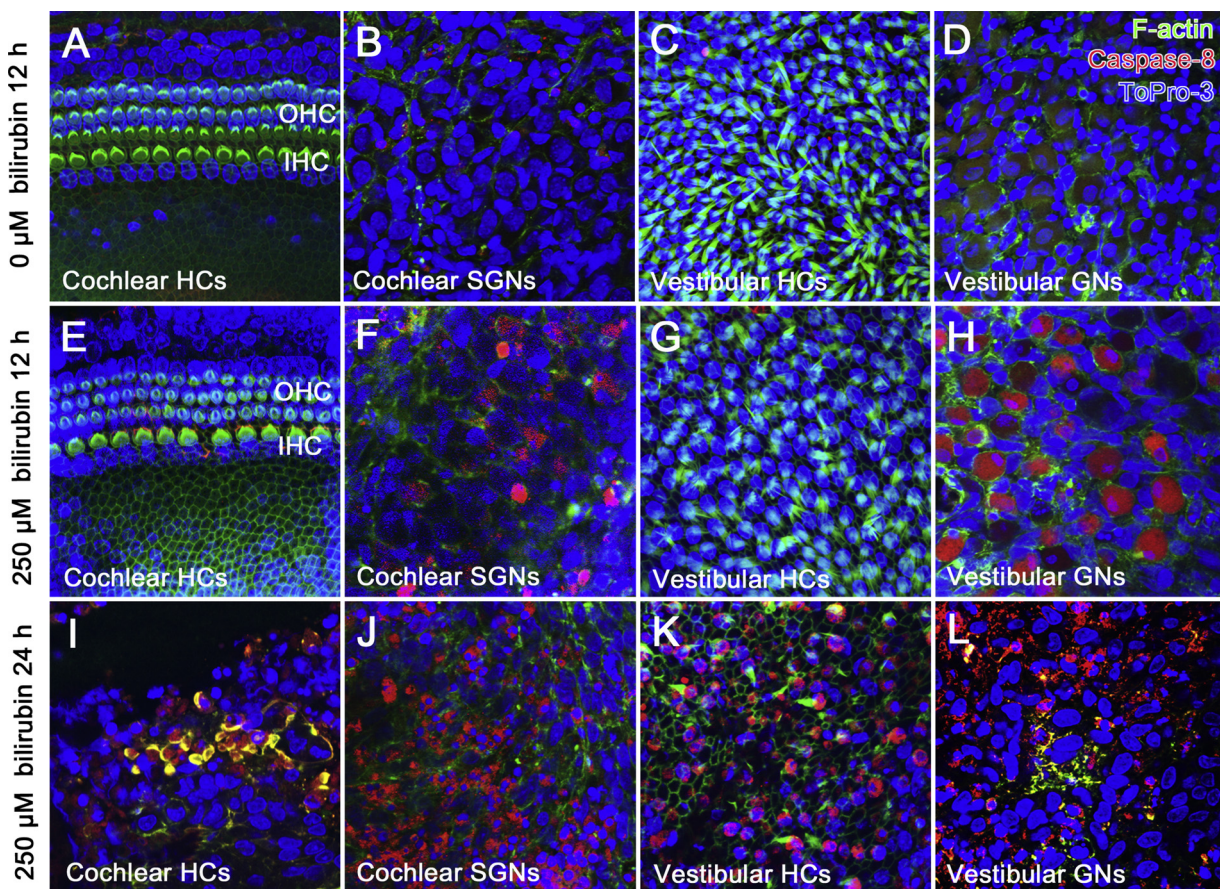


Fig. 6. Photomicrographs showing the bilirubin-induced activation of caspase-8 in the control group and cultures treated with 250 µM bilirubin for 12 or 24 h. Caspase-8 was absent in the normal control cochlear and vestibular sensory epithelium and peripheral GNs (A–D). At 12 h after treatment with 250 µM bilirubin, caspase-8 was intensely expressed in SGNs and VGNs but there was no activation in the cochlear and vestibular sensory HCs (E–H). At 24 h after treatment with 250 µM bilirubin, caspase-8 activation was detected in all cochlear and vestibular sensory HCs and their peripheral GNs (I–L). Caspase-8 was shown in red. F-actin on stereocilia was stained with phalloidin (green). Nuclei were stained with ToPro-3 (blue).

(DPOAEs) or CM, which are thought to be produced by cochlear OHCs. Therefore, the results of current *in vitro* experimental studies can be supplemented to support our previous findings *in vivo*. Although the concentration of bilirubin in the inner ear fluid has not been detected yet, but according to bilirubin exposure rapidly and effectively causes functional changes in cochlear bioelectricities with pathological changes in auditory nerve endings and nerve fibers, bilirubin is considered to be able to cross the blood-labyrinth barrier to exert its neurotoxic effect in the inner ear (Ye et al., 2012, 2013). In the present study, the bilirubin-induced destruction of cochlear HCs occurred at the highest dose (250 µM), which indicates that the resistance of HCs did not persist if the bilirubin dose was extremely high. Therefore, it is believed that hyperbilirubinemia could lead to ANSD and the pathological site(s) of dysfunction that could distinguish these disorders may be located in peripheral cochlear end-organs.

The present results concerning vestibular toxicity were particularly interesting. Few studies have evaluated the effects of hyperbilirubinemia on vestibular function but Nash (Nash et al., 2014) found that vestibulopathy is relatively prevalent in pediatric ANSD patients, especially in those with neonatal jaundice. These authors proposed that the mechanisms underlying ANSD most likely include vestibulocochlear nerve dysfunction. To the best of our knowledge, the present study was the first to show that bilirubin-induced damage occurs in vestibular end-organs and vestibular GNs in organotypic cultures. Similar to the cochlea, the destruction of vestibular HCs was obvious only at the highest bilirubin dose (250 µM) and, therefore, it will be important to screen for vestibulopathy in ANSD patients. When considering the location of a ‘lesion’ that causes ANSD, a more generalized or central

process may predispose one to concomitant vestibulopathy while also negatively affecting the outcomes of cochlear implantation. Previous studies have indicated that ANSD patients are more likely to exhibit damage in the inferior vestibular nerve and saccule than the superior vestibular nerve or semicircular canals (Sazgar et al., 2010; Sinha et al., 2013). Given that this result was experimentally induced, it suggests that the presence of vestibulopathy in many ANSD patients could be indicative of a vestibulocochlear neuropathy. However, the extent and significance of these findings should be further investigated in additional studies.

The neuronal susceptibility to bilirubin encompasses a spectrum of phenotypes that ranges from impairments in cellular morphology to death (Watchko and Tiribelli, 2013). Bilirubin toxicity is involved in the disruption of neuronal energy metabolism (which is associated with apoptosis- and necrosis-like cell death), and is mediated by the early signals of endoplasmic reticulum stress and mitochondrial dysfunction; this results in an energy crisis that ultimately releases multiple apoptotic signals (Barateiro et al., 2012; Kuter et al., 2018; Ostrow et al., 2004; Vodret et al., 2018; Watchko, 2016). A variety of mechanisms such as excitotoxicity, oxidative/nitrosative processes, hyperexcitation that occurs via the potentiation of presynaptic glutamate release from free radicals after injury, and microglial activation in conjunction with the consequent inflammatory response have been implicated in neuronal cellular injury and death (Back and Rosenberg, 2014; Brites, 2012; Li et al., 2011a, b; Liang et al., 2017a). The present study demonstrated that many SGNs and VGNs exhibited condensed, fragmented, or shrunken structures in conjunction with positive caspase labeling (two initiators [caspase-8 and caspase-9] and one executioner

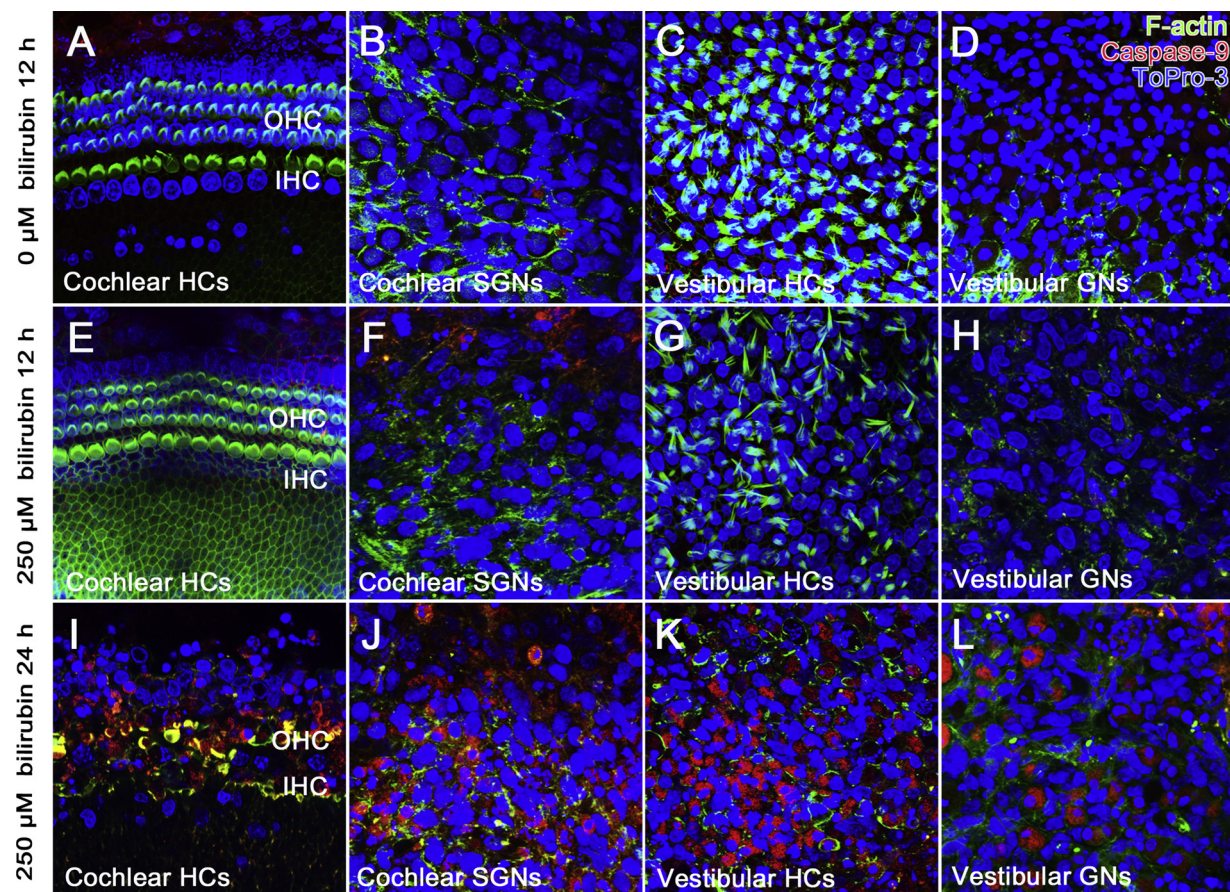


Fig. 7. Photomicrographs showing the bilirubin-induced activation of caspase-9 in the control group and cultures treated with 250 μM bilirubin for 12 or 24 h. Caspase-9 was not detected in cochlear and vestibular HCs in the normal control group or at 12 h after treatment with 250 μM bilirubin (A–H). Activated caspase-9 was expressed in all cochlear and vestibular sensory HCs and their GNs at 24 h after treatment with 250 μM bilirubin (I–L). Caspase-9 was shown in red. F-actin on stereocilia was stained with phalloidin (green). Nuclei were stained with ToPro-3 (blue).

[caspase-3]) after 12 and 24 h of culturing with high doses of bilirubin.

Caspases, which are members of a family of cysteine-dependent aspartate-specific proteases, play an important role in programmed cell death. The specific caspases involved in apoptosis vary by cell type and mode of injury (Samali et al., 1999). Caspase-8 and -9 represent two major pathways that initiate cell death and both lie upstream of caspase-3, which is an executioner (Chinnaiyan et al., 1995; Hsu et al., 1995). Caspase-9-mediated cell destruction is initiated through mitochondrial damage that leads to the release of cytochrome C into the cytosol (Krajewski et al., 1999). The present results also showed that the activations of caspase-3 and -8 occurred in cochlear and vestibular GNs but not cochlear and vestibular sensory HCs whereas caspase-9 was not detected in either cochlear or vestibular SGNs at 12 h after treatment with 250 μM bilirubin. At 24 h after treatment with 250 μM bilirubin, the activations of all three caspases were detected in all cochlear and vestibular sensory HCs as well as their peripheral SGNs. Thus, these results indicate that bilirubin-induced SGN death mostly occurred via apoptosis.

These apoptotic signals were initiated by extrinsic caspase-8, which may be released from tumor necrosis factor receptors on the membrane surface and may be followed by the activation of caspase-3. Because caspase-9 activation only responds to a complex of cytochrome C and apoptotic protease activating factor 1 (APAF-1), caspase-9 activity occurs only after 24 h of treatment with 250 μM bilirubin. This time point is towards the end of apoptosis and, thus, the intrinsic apoptotic pathway may not be a major factor. Because caspase-8 exhibits early activity, bilirubin-induced apoptosis most likely occurs through the extrinsic apoptotic pathway. However, the exact apoptotic pathways

and degenerative mechanisms activated by bilirubin treatment in cochlear and vestibular organotypic cultures remain unclear.

During neonatal hyperbilirubinemia, toxicity occurs in the presence of high levels of unconjugated bilirubin (UCB), usually $> 342 \mu\text{M}$, and after long periods of exposure (Silva et al., 2001). Furthermore, bilirubin neurotoxicity is determined by the free fraction of UCB, which can easily cross the blood-brain barrier to exert toxic effects (Amin et al., 2001; Wennberg, 2000). However, the manner in which free bilirubin permeates the blood-labyrinth barrier to cause toxic effects in the inner ear remains unclear. Other factors, including acidosis and competitors of bilirubin binding to albumin, may also increase the interaction of bilirubin with cells and neurons (Brodersen and Stern, 1990). Moreover, the complex and multifactorial nature of this disorder continues to hinder the identification of a neurotoxic threshold for bilirubin as well as the accurate predictions of clinical cases of bilirubin encephalopathy and hearing loss (Watchko and Tiribelli, 2013). Nevertheless, the present findings indicate that the application of bilirubin concentrations in the range of 10–250 μM to rat cochlear and vestibular organotypic cultures can induce neurotoxicity, which suggests these doses are likely to cause hearing loss in neonates with clinical hyperbilirubinemia. Despite the present efforts regarding the use of inner ear organotypic cultures to assess bilirubin-induced neurotoxicity, neither a robust unifying hypothesis nor a consensus model of bilirubin neurotoxicity has been firmly established. Thus, basic research endeavors must strive to fully integrate the insights obtained from *in vitro* (cell lines, co-culture systems, and slice preparations) and *in vivo* (murine models) investigations with those observed in human neonates (neuropathology and neuroimaging) to distinguish causal relationships from an

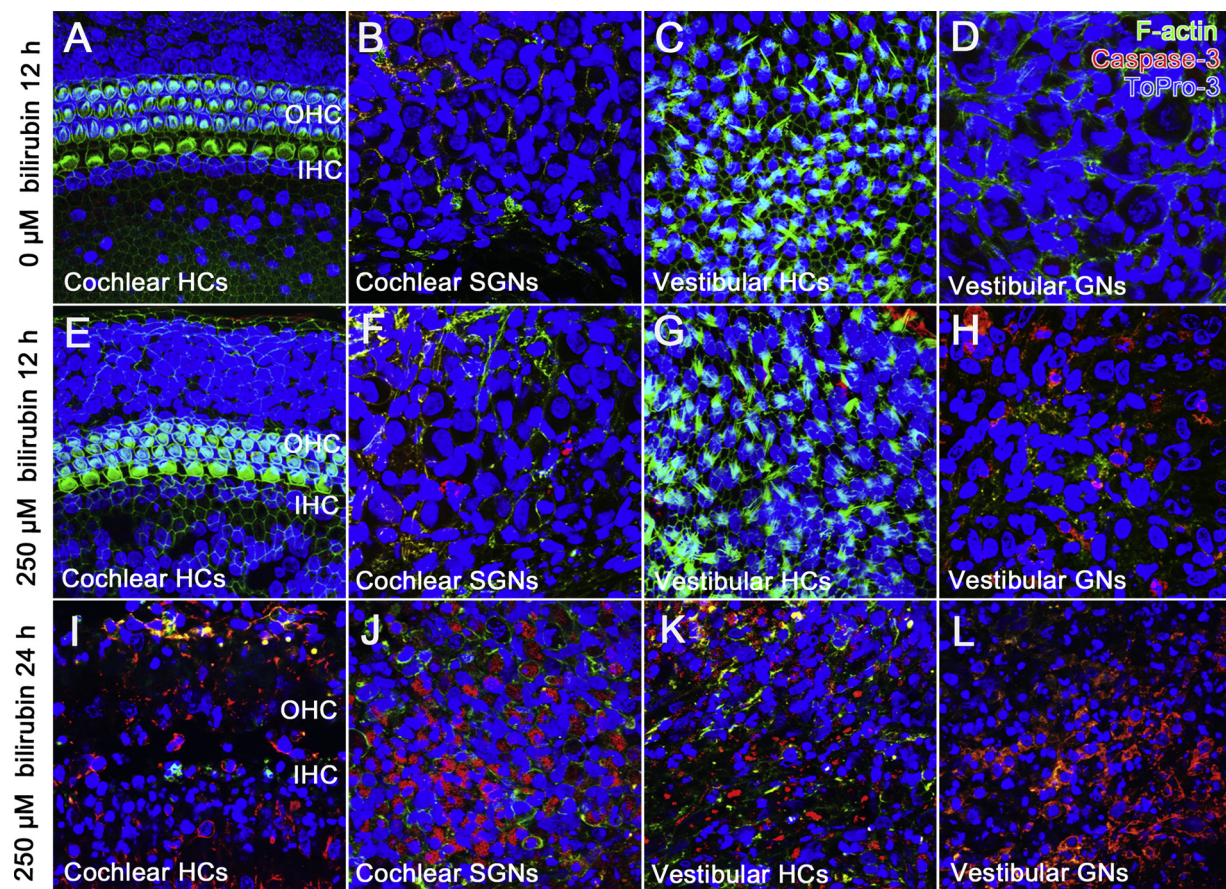


Fig. 8. Photomicrographs showing the bilirubin-induced activation of caspase-3 in the control group and cultures treated with 250 μ M bilirubin for 12 or 24 h. Caspase-3 activation was absent in the normal control cochlear and vestibular sensory epithelium and peripheral GNs (A–D). At 12 h after treatment with 250 μ M bilirubin, caspase-3 activation was detected in SGNs and VGNs but not cochlear and vestibular sensory HCs (F–H). At 24 h after treatment with 250 μ M bilirubin, caspase-3 activation was detected in all cochlear and vestibular sensory HCs and their peripheral GNs (I–L). Caspase-3 was shown in red. F-actin on stereocilia was stained with phalloidin (green). Nuclei were stained with ToPro-3 (blue).

The English in this document has been checked by at least two professional editors, both native speakers of English. For a certificate, please see: <http://www.textcheck.com/certificate/AhDrB9>.

epiphenomenon (Watchko, 2016).

According to the results from current experiment, it can be determined that the toxic effects of bilirubin to the cochlea and vestibular neurons occur earlier and more severe than the toxic effects to the sensory HCs in the inner ear. The absorption of bilirubin by cells is mainly through the diffusion. Bilirubin-induced cellular caspase cascade was initiated from the caspase-8. Since the caspase-8 is the initial caspase activated in response to receptors with a death domain on cell membrane that interacts with FADD, therefore, the activation of caspase-8 is considered as a marker of extrinsic apoptosis. In view of the fact that many ototoxic drugs can cause cell apoptosis in the inner ear, the neurotoxicity and ototoxicity of bilirubin appear to have some similarities with other ototoxic drugs such as aminoglycoside antibiotics or anti-tumor platinum agents. However, the toxic process and mechanism of bilirubin may differ from other ototoxic drugs. As a representative of aminoglycoside antibiotics, gentamicin can selectively bind to the mitochondrial ribosome at the A (adenosine) decoding region of 16 S ribosomal RNA (rRNA) by active transport rather than diffusion. Since mitochondria participate in protein synthesis through 70 S ribosomes and are abundantly expressed in HCs, sensory HCs in the inner ear become the major target of gentamicin and are preferentially destroyed, while the HC loss eventually leads to subsequent helical secondary degeneration of SGNs (Ding et al., 1995, 1997). Gentamicin-induced apoptotic signal release is a complex of cytochrome c and apaf-1 with dATP, which results in activation of promoter caspase-9 and then activates the executioner caspase-3. Therefore,

gentamicin-induced HC apoptosis is an intrinsic typical mitochondrial apoptotic pathway (Ding et al., 2010). In comparison with the bilirubin-induced specific destruction to peripheral neurons and extrinsic apoptotic pathway with the gentamicin-induced preferential damage to sensory HCs and intrinsic apoptotic pathway, obviously, the attack targets and destruction processes and the apoptotic mechanisms of these two chemicals are completely different. As a representative of anti-tumor platinum agents, cisplatin can only exert its toxic effects when it enters the cytoplasm through a copper transport channel, and its chlorine atoms are replaced by water molecules and bind to glutathione in the cytoplasm (Ding et al., 2011a; Hanigan et al., 2001). Cisplatin-induced cell apoptosis occurs simultaneously in sensory HCs and peripheral neurons as well as in surrounding support cells in the inner ear. Cisplatin-induced apoptosis signal is released from the cell death receptors on the cell membrane, which leads to the activation of initiator caspase-8, and followed by activation of executioner caspase-3 and triggering of p53 apoptotic pathway (Ding et al., 2012b, a; Ding et al., 2007). Although both bilirubin and cisplatin can induce extrinsic apoptosis, base on our current experiment, we found that bilirubin specifically damages the peripheral GNs in the inner ear, and can also destroy the sensory HCs by very high doses of bilirubin treatment, but rarely damage the supporting cells (Ding et al., 2012a, a; He et al., 2011). In addition, cisplatin enter cells via copper transporters, however, bilirubin does not enter cells through the copper transporters (Kalakonda and John, 2018). Therefore, bilirubin-induced toxic pathway and the process of injury may not be exactly the same as

cisplatin.

5. Conclusions

In summary, the present study applied various doses of bilirubin to cochlear and vestibular organotypic cultures and presented the first evidence showing that damage to HCs, SGNs, ANFs, and synapses in cochlear and vestibular organs varies based on different levels of extracellular bilirubin. Additionally, the present study revealed the time course and pattern of bilirubin-induced ototoxicity via analyses of different markers of apoptosis and showed that bilirubin-induced major apoptosis most likely occurs through the extrinsic apoptotic pathway. The present study was conducted in an effort to fully establish a dose-response curve for bilirubin-induced ototoxicity in postnatal cochlear and vestibular cultures but further work will be necessary to elucidate fully the mechanisms underlying bilirubin neurotoxicity in SGNs and ANFs. Furthermore, the issue of protection against this type of neurotoxicity should be addressed in future studies using organ cultures from the inner ear and the vestibular system where it is possible to apply a wide range of bilirubin concentrations. From a clinical perspective, the present results suggest that bilirubin could be extremely toxic to cochlear and vestibular nerve architecture and may represent possible mechanisms underlying ANSD and vestibulopathy.

Declarations of interest

None.

Acknowledgments

This work was supported by the Funds for International Cooperation and Exchange of the National Natural Science Foundation of China [grant number 81720108010]; the State Key Program of National Natural Science of China [grant number 81530029]; the National Natural Science Foundation of China [grant numbers 81470690, 81570909, 81870722]; and Shanghai leadership talent training plan [grant number 2017062].

References

- Ahdab-Barmada, M., Moosy, J., 1984. The neuropathology of kernicterus in the premature neonate: diagnostic problems. *J. Neuropathol. Exp. Neurol.* 43 (1), 45–56.
- Ahlfors, C.E., Shapiro, S.M., 2001. Auditory brainstem response and unbound bilirubin in jaundiced (jj) Gunn rat pups. *Biol. Neonate* 80 (2), 158–162.
- Amin, S.B., Ahlfors, C., Orlando, M.S., Dalzell, L.E., Merle, K.S., Guillet, R., 2001. Bilirubin and serial auditory brainstem responses in premature infants. *Pediatrics* 107 (4), 664–670.
- Back, S.A., Rosenberg, P.A., 2014. Pathophysiology of glia in perinatal white matter injury. *Glia* 62 (11), 1790–1815.
- Barateiro, A., Vaz, A.R., Silva, S.L., Fernandes, A., Brites, D., 2012. ER stress, mitochondrial dysfunction and calpain/JNK activation are involved in oligodendrocyte precursor cell death by unconjugated bilirubin. *Neuromolecular. Med.* 14 (4), 285–302.
- Belal Jr, A., 1975. Effect of hyperbilirubinemia on the inner ear in Gunn rats. *J. Laryngol. Otol.* 89 (3), 259–265.
- Bhutani, V.K., Wong, R.J., 2013. Bilirubin neurotoxicity in preterm infants: risk and prevention. *J. Clin. Neonatol.* 2 (2), 61–69.
- Brites, D., 2012. The evolving landscape of neurotoxicity by unconjugated bilirubin: role of glial cells and inflammation. *Front Pharmacol.* 3, 88.
- Brodersen, R., Stern, L., 1990. Deposition of bilirubin acid in the central nervous system—a hypothesis for the development of kernicterus. *Acta Paediatr. Scand.* 79 (1), 12–19.
- Chinnaiyan, A.M., O'Rourke, K., Tewari, M., Dixit, V.M., 1995. FADD, a novel death domain-containing protein, interacts with the death domain of Fas and initiates apoptosis. *Cell* 81 (4), 505–512.
- Dalian, D., Haiyan, J., Yong, F., Yongqi, L., Salvi, R., Someya, S., Tanokura, M., 2013. Ototoxic model of oxaliplatin and protection from nicotinamide adenine dinucleotide. *J. Otol.* 8 (1), 63–71.
- Dennery, P.A., Seidman, D.S., Stevenson, D.K., 2001. Neonatal hyperbilirubinemia. *N. Engl. J. Med.* 344 (8), 581–590.
- Ding, D., Jin, X., Zhao, J., 1995. [Accumulation sites of kanamycin in cochlear basal membrane cells]. *Zhonghua Er Bi Yan Hou Ke Za Zhi* 30 (6), 323–325.
- Ding, D., Jin, X., Zhao, J., 1997. [Accumulation sites of kanamycin in the organ of Corti by microautoradiography]. *Zhonghua Er Bi Yan Hou Ke Za Zhi* 32 (6), 348–349.
- Ding, D., Stracher, A., Salvi, R.J., 2002. Leupeptin protects cochlear and vestibular hair cells from gentamicin ototoxicity. *Hear. Res.* 164 (1–2), 115–126.
- Ding, D., Jiang, H., Wang, P., Salvi, R., 2007. Cell death after co-administration of cisplatin and ethacrynic acid. *Hear. Res.* 226 (1–2), 129–139.
- Ding, D., Jiang, H., Salvi, R.J., 2010. Mechanisms of rapid sensory hair-cell death following co-administration of gentamicin and ethacrynic acid. *Hear. Res.* 259 (1–2), 16–23.
- Ding, D., He, J., Allman, B.L., Yu, D., Jiang, H., Seigel, G.M., Salvi, R.J., 2011a. Cisplatin ototoxicity in rat cochlear organotypic cultures. *Hear. Res.* 282 (1–2), 196–203.
- Ding, D., Roth, J., Salvi, R., 2011b. Manganese is toxic to spiral ganglion neurons and hair cells in vitro. *Neurotoxicology* 32 (2), 233–241.
- Ding, D., Allman, B.L., Salvi, R., 2012a. Review: ototoxic characteristics of platinum antitumor drugs. *Anat. Rec. (Hoboken)* 295 (11), 1851–1867.
- Ding, D., Haiyan, J., Yong, F., Salvi, R., Someya, S., Tanokura, M., 2012b. Ototoxic effects of carboplatin in organotypic cultures in chinchillas and rats. *J. Otol.* 7 (2), 92–101.
- Dong, Y., Ding, D., Jiang, H., Shi, J.R., Salvi, R., Roth, J.A., 2014. Ototoxicity of paclitaxel in rat cochlear organotypic cultures. *Toxicol. Appl. Pharmacol.* 280 (3), 526–533.
- Fu, Y., Ding, D., Wei, L., Jiang, H., Salvi, R., 2013. Ouabain-induced apoptosis in cochlear hair cells and spiral ganglion neurons in vitro. *Biomed. Res. Int.*, 628064.
- Gao, K., Ding, D., Sun, H., Roth, J., Salvi, R., 2017. Kanamycin damages early postnatal, but not adult spiral ganglion neurons. *Neurotox. Res.* 32 (4), 603–613.
- Gupta, A.K., Mann, S.B., 1998. Is auditory brainstem response a bilirubin neurotoxicity marker? *Am. J. Otolaryngol.* 19 (4), 232–236.
- Hanigan, M.H., Lykissa, E.D., Townsend, D.M., Ou, C.N., Barrios, R., Lieberman, M.W., 2001. Gamma-glutamyl transpeptidase-deficient mice are resistant to the nephrotoxic effects of cisplatin. *Am. J. Pathol.* 159 (5), 1889–1894.
- He, J., Ding, D., Yu, D., Jiang, H., Yin, S., Salvi, R., 2011. Modulation of copper transporters in protection against cisplatin-induced cochlear hair cell damage. *J. Otol.* 6 (6), 53–61.
- Hrnčic, N., 2018. Identification of risk factors for hearing impairment in newborns: a hospital based study. *Med. Glas (Zenica)* 15 (1), 29–36.
- Hsu, H., Xiong, J., Goeddel, D.V., 1995. The TNF receptor 1-associated protein TRADD signals cell death and NF- κ B activation. *Cell* 81 (4), 495–504.
- Jeffery, N., Spoor, F., 2004. Prenatal growth and development of the modern human labyrinth. *J. Anat.* 204 (2), 71–92.
- Jiang, Z.D., Chen, C., Liu, T.T., Wilkinson, A.R., 2007. Changes in brainstem auditory evoked response latencies in term neonates with hyperbilirubinemia. *Pediatr. Neurol.* 37 (1), 35–41.
- Kalakonda, A., John, S., 2018. Physiology, Bilirubin. *StatPearls*, Treasure Island (FL).
- Krajewski, S., Krajewska, M., Ellerby, L.M., Welsh, K., Xie, Z., Deveraux, Q.L., Salvesen, G.S., Bredesen, D.E., Rosenthal, R.E., Fiskum, G., Reed, J.C., 1999. Release of caspase-9 from mitochondria during neuronal apoptosis and cerebral ischemia. *Proc. Natl. Acad. Sci. U. S. A.* 96 (10), 5752–5757.
- Kuter, N., Aysit-Altuncu, N., Ozturk, G., Ozek, E., 2018. The neuroprotective effects of hypothermia on bilirubin-induced neurotoxicity in vitro. *Neonatology* 113 (4), 360–365.
- Li, C.Y., Shi, H.B., Song, N.Y., Yin, S.K., 2011a. Bilirubin enhances neuronal excitability by increasing glutamatergic transmission in the rat lateral superior olive. *Toxicology* 284 (1–3), 19–25.
- Li, C.Y., Shi, H.B., Wang, J., Ye, H.B., Song, N.Y., Yin, S.K., 2011b. Bilirubin facilitates depolarizing GABA/glycinergic synaptic transmission in the ventral cochlear nucleus of rats. *Eur. J. Pharmacol.* 660 (2–3), 310–317.
- Li, C.Y., Shi, H.B., Ye, H.B., Song, N.Y., Yin, S.K., 2012. Minocycline cannot protect neurons against bilirubin-induced hyperexcitation in the ventral cochlear nucleus. *Exp. Neurol.* 237 (1), 96–102.
- Li, P., Ding, D., Salvi, R., Roth, J.A., 2015. Cobalt-induced ototoxicity in rat postnatal cochlear organotypic cultures. *Neurotox. Res.* 28 (3), 209–221.
- Liang, M., Yin, X.L., Shi, H.B., Li, C.Y., Li, X.Y., Song, N.Y., Shi, H.S., Zhao, Y., Wang, L.Y., Yin, S.K., 2017a. Bilirubin augments Ca(2+) load of developing bushy neurons by targeting specific subtype of voltage-gated calcium channels. *Sci. Rep.* 7 (1), 431.
- Liang, M., Yin, X.L., Wang, L.Y., Yin, W.H., Song, N.Y., Shi, H.B., Li, C.Y., Yin, S.K., 2017b. NAD+ attenuates bilirubin-induced hyperexcitation in the ventral cochlear nucleus by inhibiting excitatory neurotransmission and neuronal excitability. *Front. Cell. Neurosci.* 11, 21.
- Madden, C., Rutter, M., Hilbert, L., Greinwald Jr, J.H., Choo, D.I., 2002. Clinical and audiological features in auditory neuropathy. *Arch. Otolaryngol. Head. Neck Surg.* 128 (9), 1026–1030.
- Maisels, M.J., McDonagh, A.F., 2008. Phototherapy for neonatal jaundice. *N. Engl. J. Med.* 358 (9), 920–928.
- Moser, T., Starr, A., 2016. Auditory neuropathy–neural and synaptic mechanisms. *Nat. Rev. Neurol.* 12 (3), 135–149.
- Nash, R., Veness, J., Wyatt, M., Raglan, E., Rajput, K., 2014. Vestibular function in children with auditory neuropathy spectrum disorder. *Int. J. Pediatr. Otorhinolaryngol.* 78 (8), 1269–1273.
- Olds, C., Oghalai, J.S., 2015. Audiologic impairment associated with bilirubin-induced neurologic damage. *Semin. Fetal. Neonatal. Med.* 20 (1), 42–46.
- Ostrow, J.D., Pascolo, L., Brites, D., Tiribelli, C., 2004. Molecular basis of bilirubin-induced neurotoxicity. *Trends Mol. Med.* 10 (2), 65–70.
- Oysu, C., Aslan, I., Ulubil, A., Baserer, N., 2002. Incidence of cochlear involvement in hyperbilirubinemic deafness. *Ann. Otol. Rhinol. Laryngol.* 111 (11), 1021–1025.
- Ozkiran, S., Gokmen, Z., Ecevit, A., Erbek, S., Erbek, S.S., Ozel, D., Tarcan, A., 2012. Vestibular evoked myogenic potentials in term newborn infants with severe hyperbilirubinemia. *Pediatr. Int.* 54 (5), 646–650.
- Perlman, M., Fainmesser, P., Sohmer, H., Tamari, H., Wax, Y., Pevsner, B., 1983. Auditory nerve-brainstem evoked responses in hyperbilirubinemic neonates. *Pediatrics* 72 (5), 658–664.

- Rance, G., 2005. Auditory neuropathy/dys-synchrony and its perceptual consequences. *Trends Amplif.* 9 (1), 1–43.
- Rance, G., Starr, A., 2015. Pathophysiological mechanisms and functional hearing consequences of auditory neuropathy. *Brain* 138 (Pt 11), 3141–3158.
- Rance, G., Beer, D.E., Cone-Wesson, B., Shepherd, R.K., Dowell, R.C., King, A.M., Rickards, F.W., Clark, G.M., 1999. Clinical findings for a group of infants and young children with auditory neuropathy. *Ear Hear.* 20 (3), 238–252.
- Reichman, N.E., Teitler, J.O., Moullin, S., Ostfeld, B.M., Hegyi, T., 2015. Late-preterm birth and neonatal morbidities: population-level and within-family estimates. *Ann. Epidemiol.* 25 (2), 126–132.
- Rhee, C.K., Park, H.M., Jang, Y.J., 1999. Audiologic evaluation of neonates with severe hyperbilirubinemia using transiently evoked otoacoustic emissions and auditory brainstem responses. *Laryngoscope* 109 (12), 2005–2008.
- Rice, A.C., Shapiro, S.M., 2006. Biliverdin-induced brainstem auditory evoked potential abnormalities in the jaundiced Gunn rat. *Brain Res.* 1107 (1), 215–221.
- Saluja, S., Agarwal, A., Kler, N., Amin, S., 2010. Auditory neuropathy spectrum disorder in late preterm and term infants with severe jaundice. *Int. J. Pediatr. Otorhinolaryngol.* 74 (11), 1292–1297.
- Samali, A., Zhivotovsky, B., Jones, D., Nagata, S., Orrenius, S., 1999. Apoptosis: cell death defined by caspase activation. *Cell. Death Differ.* 6 (6), 495–496.
- Sano, M., Kaga, K., Kitazumi, E., Kodama, K., 2005. Sensorineural hearing loss in patients with cerebral palsy after asphyxia and hyperbilirubinemia. *Int. J. Pediatr. Otorhinolaryngol.* 69 (9), 1211–1217.
- Sazgar, A.A., Yazdani, N., Rezazadeh, N., Yazdi, A.K., 2010. Vestibular evoked myogenic potential (VEMP) in patients with auditory neuropathy: auditory neuropathy or audiovestibular neuropathy? *Acta Otolaryngol.* 130 (10), 1130–1134.
- Shaia, W.T., Shapiro, S.M., Spencer, R.F., 2005. The jaundiced Gunn rat model of auditory neuropathy/dysynchrony. *Laryngoscope* 115 (12), 2167–2173.
- Shapiro, S.M., 1994. Brainstem auditory evoked potentials in an experimental model of bilirubin neurotoxicity. *Clin. Pediatr. (Phila)* 33 (8), 460–467.
- Shapiro, S.M., Nakamura, H., 2001. Bilirubin and the auditory system. *J. Perinatol.* 21 (Suppl. 1) S52–S55; discussion S59–62.
- Shapiro, S.M., Popelka, G.R., 2011. Auditory impairment in infants at risk for bilirubin-induced neurologic dysfunction. *Semin. Perinatol.* 35 (3), 162–170.
- Sharma, P., Chhangani, N.P., Meena, K.R., Jora, R., Sharma, N., Gupta, B.D., 2006. Brainstem evoked response audiometry (BAER) in neonates with hyperbilirubinemia. *Indian J. Pediatr.* 73 (5), 413–416.
- Sheykholeslami, K., Kaga, K., 2000. Otoacoustic emissions and auditory brainstem responses after neonatal hyperbilirubinemia. *Int. J. Pediatr. Otorhinolaryngol.* 52 (1), 65–73.
- Shi, H.B., Kakazu, Y., Shibata, S., Matsumoto, N., Nakagawa, T., Komune, S., 2006. Bilirubin potentiates inhibitory synaptic transmission in lateral superior olive neurons of the rat. *Neurosci. Res.* 55 (2), 161–170.
- Silva, R.F., Rodrigues, C.M., Brites, D., 2001. Bilirubin-induced apoptosis in cultured rat neural cells is aggravated by chenodeoxycholic acid but prevented by ursodeoxycholic acid. *J. Hepatol.* 34 (3), 402–408.
- Sinha, S.K., Barman, A., Singh, N.K., Rajeshwari, G., Sharanya, R., 2013. Involvement of peripheral vestibular nerve in individuals with auditory neuropathy. *Eur. Arch. Otorhinolaryngol.* 270 (8), 2207–2214.
- Starr, A., Picton, T.W., Sininger, Y., Hood, L.J., Berlin, C.I., 1996. Auditory neuropathy. *Brain* 119 (Pt 3), 741–753.
- Vodret, S., Bortolussi, G., Iaconig, A., Martinelli, E., Tiribelli, C., Muro, A.F., 2018. Attenuation of neuro-inflammation improves survival and neurodegeneration in a mouse model of severe neonatal hyperbilirubinemia. *Brain Behav. Immun.* 70, 166–178.
- Wang, L., Ding, D., Salvi, R., Roth, J.A., 2014. Nicotinamide adenine dinucleotide prevents neuroaxonal degeneration induced by manganese in cochlear organotypic cultures. *Neurotoxicology* 40, 65–74.
- Watchko, J.F., 2006. Neonatal hyperbilirubinemia—what are the risks? *N. Engl. J. Med.* 354 (18), 1947–1949.
- Watchko, J.F., 2016. Bilirubin-induced neurotoxicity in the preterm neonate. *Clin. Perinatol.* 43 (2), 297–311.
- Watchko, J.F., Tiribelli, C., 2013. Bilirubin-induced neurologic damage—mechanisms and management approaches. *N. Engl. J. Med.* 369 (21), 2021–2030.
- Watson, R.L., 2009. Hyperbilirubinemia. *Crit. Care Nurs. Clin. North. Am.* 21 (1), 97–120 vii.
- Wei, L., Ding, D., Salvi, R., 2010. Salicylate-induced degeneration of cochlea spiral ganglion neurons-apoptosis signaling. *Neuroscience* 168 (1), 288–299.
- Wennberg, R.P., 2000. The blood-brain barrier and bilirubin encephalopathy. *Cell Mol. Neurobiol.* 20 (1), 97–109.
- Ye, H.B., Shi, H.B., Wang, J., Ding, D.L., Yu, D.Z., Chen, Z.N., Li, C.Y., Zhang, W.T., Yin, S.K., 2012. Bilirubin induces auditory neuropathy in neonatal guinea pigs via auditory nerve fiber damage. *J. Neurosci. Res.* 90 (11), 2201–2213.
- Ye, H.B., Wang, J., Zhang, W.T., Shi, H.B., Yin, S.K., 2013. Taurine attenuates bilirubin-induced neurotoxicity in the auditory system in neonatal guinea pigs. *Int. J. Pediatr. Otorhinolaryngol.* 77 (5), 647–654.
- Yu, D., Ding, D., Jiang, H., Stolzberg, D., Salvi, R., 2011. Mefloquine damage vestibular hair cells in organotypic cultures. *Neurotox. Res.* 20 (1), 51–58.
- Yu, J., Ding, D., Sun, H., Salvi, R., Roth, J.A., 2015. Neurotoxicity of trimethyltin in rat cochlear organotypic cultures. *Neurotox. Res.* 28 (1), 43–54.
- Zhou, Y., Ding, D., Kraus, K.S., Yu, D., Salvi, R.J., 2009. Functional and structural changes in the chinchilla cochlea and vestibular system following round window application of carboplatin. *Audiol. Med.* 7 (4), 189–199.